

Potential application of graphene nanoplatelets as a high temperature lubricant for hot rolling

Long WANG^{1,2}, Anh Kiet TIEU^{2,*}, Ming MA³, Jiaqing LI², Guojuan HAI⁴, Hongtao ZHU^{2,*}

¹ State Key Laboratory of Solidification Processing, Center of Advanced Lubrication and Seal Materials, Northwestern Polytechnical University, Xi'an 710021, China

² School of Mechanical, Materials, Mechatronic and Biomedical Engineering, Faculty of Engineering and Information Sciences, University of Wollongong, Northfields Avenue, Wollongong, NSW 2522, Australia

³ State Key Laboratory of Tribology, Department of Mechanical Engineering, Tsinghua University, Beijing 100084, China

⁴ School of Materials Science and Engineering, Shaanxi University of Science and Technology, Xi'an 710021, China

Received: 01 July 2021 / Revised: 20 August 2021 / Accepted: 20 September 2021

© The author(s) 2021.

Abstract: Graphene has been shown to be a promising solid lubricant to reduce friction and wear of the sliding counterparts, and currently is reported to only function below 600 °C. In this study, its potential as a lubricant above 600 °C was studied using a ball-on-disc tribo-meter and a rolling mill. Friction results suggest that a reduction up to 50% can be obtained with graphene nanoplatelets (GnP) under lubricated conditions between 600 and 700 °C when compared with dry tests. and this friction reduction can last more than 3 min. At 800 and 900 °C, the friction reduction is stable for 70 and 40 s, respectively, which indicates that GnP can potentially provide an effective lubrication for hot metal forming processes. Hot rolling experiments on steel strips indicate that GnP reduces the rolling force by 11%, 7.4%, and 6.9% at 795, 890, and 960 °C, respectively. These friction reductions are attributed to the easily sheared GnP between the rubbing interfaces. A temperature higher than 600 °C will lead to the gasification of the residual graphene on the strip surface, which is believed to reduce the black contamination from traditional graphite lubricant.

Keywords: graphene; high temperature lubricant; hot rolling; tribology properties

1 Introduction

Graphene has attracted widespread attention since it was first found in 2004 [1], due to its exceptional properties, including superior mechanical strength [2], good mobility [3], high thermal conductivity [4], optical transparency [5], and hydrophobicity [6]. Thus, it is promising for many potential applications, including field-effect transistors, hydrogen storage, and ultra-capacitors. Due to its atomically thin lamellar structure with low shear strength [7], graphene has also been reported as a new emerging candidate for solid lubricants that improve the adhesion and friction between contact surfaces, thus reducing the adverse

impacts of friction on durability, efficiency, and environmental concern [8, 9].

Compared with other applications, the potential of graphene as a lubricant in hot metal forming remains poorly explored, the limited studies mainly focused on tribological behaviours of graphene at room temperature, as lubricant dispersed in solution [10–14], or as a lubricant phase in the composite [15, 16] or coating [17–19]. Berman et al. [20, 21] reported that a small amount of non-continuous graphene (2–3 sheets, 1 mg/L) on the sliding surface (0.15 mL/cm²) at room temperature can decrease the coefficient of friction (COF) from 1 to 0.15 for stainless steel test pairs in both air and dry nitrogen gas because of the

* Corresponding authors: Anh Kiet TIEU, E-mail: ktieu@uow.edu.au; Hongtao ZHU, E-mail: hongtao@uow.edu.au

easily sheared two-dimensional material at the sliding interface. Other research about graphene at high temperature mentioned that the lubricative properties of graphene start changing and diminishing above 600 °C due to its oxidation [17, 22]. Xu et al. [23] suggested that below 500 °C, TiAl-based composites produce a multilayer graphene (MLG) film that provides an easy shear sliding with low friction and wear. However between 500 and 600 °C, the lubrication performance diminishes as confirmed by Raman results. Xiao et al. [24] found that graphene nanoplatelets (GnP) play an antifriction role in NiAl based self-lubricating composites in the temperature range 100–400 °C due to the formation of a friction layer of graphene, but lose lubrication due to oxidation. So it is believed that graphene will not perform well at temperatures above 600 °C. However, for hot rolling of steels above 600 °C, where the contact time is very short for only 10^{-3} – 10^{-2} s [25, 26], we believe that this short contact time is not enough for graphene to be totally oxidized. Thus, it is likely that graphene can potentially be used as a lubricant for a number of hot metal forming processes such as hot forging, seamless pipe, and hot rolling.

Therefore, in this study, we explore the possibility of

graphene being used as a high temperature lubricant in the hot rolling process for steel. Graphene is studied as a solid lubricant on both ball-on-disc UMT configuration above 600 °C and hot rolling tests using an experimental rolling mill. Raman spectroscopic analysis of the graphene powders after heat treatment in air and the wear scar after wear test is used to explain the lubrication mechanism.

2 Experiment details

2.1 Materials

GnP purchased from XG Science company (xGnP C-500, USA) was used in the experimental work. The commercial GnP has about 6 layers in thickness, identified by both transmission electron microscopy (TEM) (Fig. 1(b)) and atomic force microscopy (AFM) (Figs. 1(c) and 1(d)). The identified layer distance for the GnP is 0.337 nm, its thickness is about 2 nm (6 layers), confirmed by the height profile of the AFM image in Fig. 1(d).

The disc and ball for the ball-on-disc tests are 316 stainless steel and GCr15 steel, respectively. Before the tests, the discs were polished to a roughness of

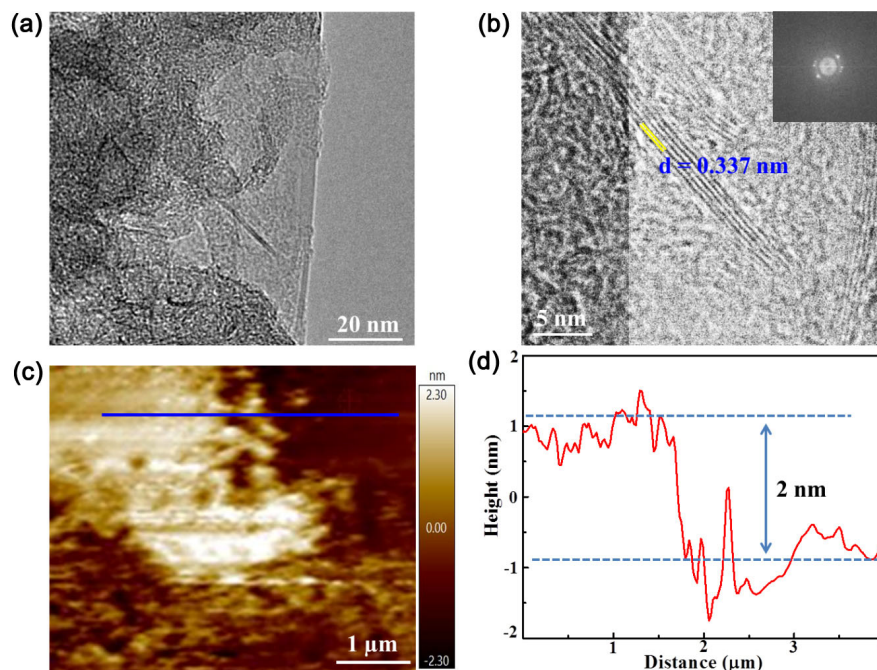


Fig. 1 (a) TEM image of the GnP; (b) high-resolution TEM (HRTEM) image of GnP and the inserted Fast Fourier Transform (FFT) image, d refers to the distance between two layers; (c) AFM image of GnP on a silicon plate surface; and (d) height profile of the marked blue line in (c).

Ra = 50 nm, measured by three-dimensional (3D) profilometer, with a diameter of 50 mm and a thickness of 3 mm. The mirror polished steel ball (GCr15 grade, Ra = 20 nm) had a diameter of 6.35 mm. Chemical compositions of the steel counterparts are listed in Table 1. The steels were initially cleaned using acetone and alcohol in a sonication bath for 10 min for contamination removal. The samples for hot rolling experiments are also 316 stainless steels, with a roughness of 0.5 μm .

2.2 Ball-on-disc tests

High temperature friction tests were carried out using a UMT tribolab machine (Bruker, USA) with a ball-on-disc contact geometry. Normal and lateral force calibration were carried out before each test to ensure the measurement reliability. At a target temperature, the lower disc rotated at a low speed of 5 r/min for 10 min to ensure thermal homogeneity and temperature stability. Then the steel ball was loaded against a rotating steel disc under the non-lubricated condition. After 3 min dry sliding, 5 mg of GnP powder was introduced into the wear tracks through a ceramic tube, and tests stopped after 3 min sliding. The ball and disc were retrieved immediately after sliding tests to minimise further oxidation. Friction tests were carried out at a sliding speed of 60 r/min (0.094 m/s) with the wear track diameter of 15 mm, and the applied load was 10 N, resulting in an initial Hertzian contact pressure of 0.8 GPa. The worn surface of the discs after friction tests were observed using a 3D profiler (Bruker, USA), and the wear volumes were calculated through the cross section area. The specific wear rate (W) is obtained by dividing wear losses (V) with applied force and sliding length. Tests were conducted at least three times to confirm the repeatability.

2.3 Hot rolling tests

To assess the effects of GnP as a lubricant for the hot

rolling process, the GnP was dispersed into distilled water to prepare 3 g/100 mL dispersion through 24 h sonication before subsequent rolling experiments. The hot rolling experiments were conducted using a 2-High Hille 100 rolling mill, with the diameter of 225 and 254 mm in length. Plates made of 316 stainless steels (200 mm (L) \times 50 mm (W) \times 10 mm (T)) were used in this study to minimise the influence of oxide scale during high temperature processing, as the stainless steel is potentially anti-oxidation with very little oxide scale formation. The specimens were reheated at 950, 1050, and 1150 $^{\circ}\text{C}$ for 25 min in a MoSi₂ tube furnace with N₂ protection gas at a rate of 15 L/min to ensure a homogeneous heat distribution and minimal oxidation scale. The rolling tests were carried out at 40 r/min (0.5 m/s) and the rolling reduction was 20%. The temperatures of the samples before entry were 795, 890, and 960 $^{\circ}\text{C}$, measured by a Micro IR-1200 non-contact infrared thermometer. The aqueous graphene solution was applied on both the roller and hot strip for the lubrication tests. For comparison, the tests with pure water as lubricant were also conducted. The rolled samples were cooled down in the cooling box with nitrogen gas inside. Hot rolling tests were carried out at least five times for each temperature.

2.4 Characterization

Raman spectrum and Raman mapping of the wear tracks and the rolled samples were collected using a HORIBA Lab RAM HR spectrometer with a laser excitation of 514 nm. A thermogravimetric analyzer (TGA) was used to identify the degradation of the used commercial GnP. It was carried out under ambient air atmosphere, with a heating rate of 20 $^{\circ}\text{C}/\text{min}$. The size and the morphologies of the worn scar with 3D contours were identified using a Contour GT-K 3D optical microscope. 3D morphologies and two-dimensional (2D) cross-sectional profile were extracted from the 3D contour by Vision64 software. A TEM (JEOL-JEM-2011, Japan) was used to assess

Table 1 Nominal composition of GCr15 and 316 stainless steel (wt%).

Element	Fe	C	Mn	Si	W	Cr	Mo	Ni	Cu
GCr15	Balance	0.98	0.27	0.35	0.1008	1.48	< 0.1	< 0.25	< 0.25
316 SS	Balance	0.037	1.88	0.4045	0.1095	18.16	1.909	11.23	0.74

the commercial GnP. A HRTEM was also adopted to identify the layer distance of the GnP. A MFP-3D AFM (Oxford Instruments company, UK) was adopted to measure the thickness of GnP.

3 Results and discussion

Frictional responses for steel-steel contact with and without GnP introduction at various temperatures are compared in Fig. 2. For the first 3 min of unlubricated (dry) sliding, the COF decreases with sliding time, this trend is attributed to progressive pickup or partial embedment of abrasive debris on the metal surface [27]. When GnP is introduced to the wear track, the COF decrease sharply from 0.67, 0.62, 0.62, and 0.4 to 0.3, 0.32, 0.4, and 0.31 for 600, 700, 800, and 900 °C, respectively. Specifically, for the tests at 600 and 700 °C, the COF is stable at around 0.32, about 50% friction reduction compared to dry test results. However, for the tests at 800 and 900 °C, the friction reduction only lasts for a short period, 70 and 40 s, respectively. Then the COF increases slightly and approaches to the unlubricated test results, which suggests that the friction is dominated by the steel–steel contact again, and GnP is totally depleted after a short duration of sliding. It can be seen from the above results that

GnP loses lubrication effectiveness after a couple of minutes supposedly due to the oxidation of GnP or consumption of GnP (burning off). The fact that lubrication effect becomes weaker above 800 °C is related to the oxidation of GnP which reduces its coverage. However, it should be noted that GnP can function for a couple of minutes, even at 900 °C, and it can potentially be used as an effective lubricant for the hot metal forming process (like hot rolling).

The specific wear rates calculated for the discs as well as the average COF are presented in Fig. 3. The average COF for the conditions with the addition of GnP is lower than the unlubricated condition for both the initial and stable period under all the temperatures. In the stable period, the average COF for GnP lubricated condition at 800 °C is higher than those at 600, 700, and 900 °C. The GnP dominates the lubrication performance between 600 and 700 °C. However, the loss of GnP at 800 °C and above left the compacted oxide scale as the main factor that influences the tribological results. A thicker, dense, and compacted oxide scale formed at a higher temperature of 900 °C is responsible for a lower COF at 900 °C compared with 800 °C. In contrast with the COF trend that decreases with test temperatures for unlubricated tests (Fig. 3(a)), the wear rate (Fig. 3(b))

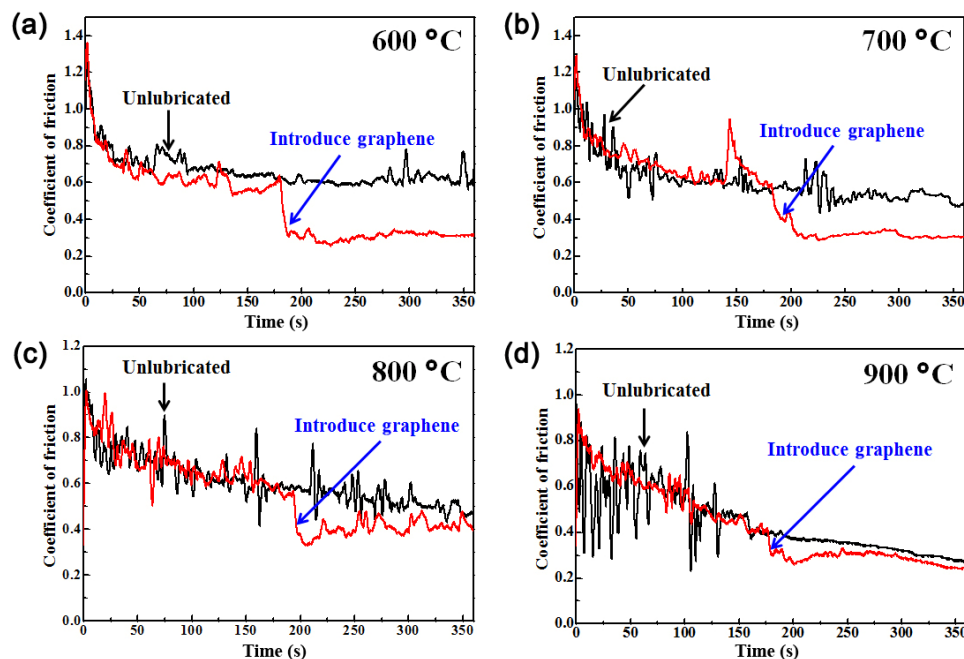


Fig. 2 COF against sliding time for dry and introduced GnP tests at various temperatures: (a) 600 °C; (b) 700 °C; (c) 800 °C; and (d) 900 °C.

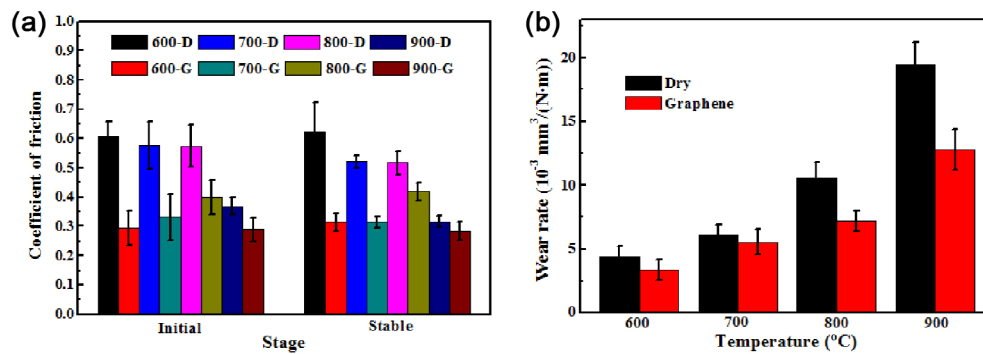


Fig. 3 (a) Average COF after GnP was introduced in the wear track for 1 min (referred to Initial stage), and average COF after 3 min (referred to stable stage) and the corresponding unlubricated test. D refers to the unlubricated condition, and G refers to the GnP lubricated condition. (b) Wear rates of the discs against temperature for both GnP lubricated and unlubricated samples.

increases with increasing temperature. Because the strength and modulus of the disc are reduce with the increase of temperature, leading to a larger area of contact and more wear, and the metals are more easily ploughed out by the harder counterpart ball. Although a large contact area leads to the increase of friction based on the thinking that the properties of the interface do not change, with the increase of temperature, more oxide wear debris will be produced, compacted, and sintered, which acts as lubricious film (glaze layer) to lower COF. It is clear that GnP can reduce the wear rate over the test temperature range. With the addition of GnP, the wear rate drops from 4.44 and $6.11 \times 10^{-3} \text{ mm}^3/(\text{N}\cdot\text{m})$ to 3.33 and $5.56 \times 10^{-3} \text{ mm}^3/(\text{N}\cdot\text{m})$ at 600 and 700 °C, respectively, and from 10.56 and $19.44 \times 10^{-3} \text{ mm}^3/(\text{N}\cdot\text{m})$ to 7.22 and $12.78 \times 10^{-3} \text{ mm}^3/(\text{N}\cdot\text{m})$ at 800 and 900 °C, respectively.

The 3D morphologies and 2D cross-sectional profile of the wear track of the discs after test at 600–900 °C were shown in Fig. 4. The size of the wear track under the unlubricated conditions is larger than that of the GnP lubricated conditions under all the temperatures. The width of the wear scar were 814.5, 929.7, 998.5, and 1,097.9 μm for the unlubricated conditions at 600, 700, 800, and 900 °C, respectively, which were 627.8, 789.1, 834.9, and 893.1 μm for the GnP lubricated conditions, respectively. The corresponding average areas of the cross-sectional profile for unlubricated conditions were are 0.0085, 0.012, 0.021, and 0.039 mm^2 , respectively, larger than that of GnP lubricated condition, which were 0.0045, 0.0085, 0.012, and 0.019 mm^2 , respectively.

These results indicate that GnP can reduce friction

and wear even up to 900 °C. This is supposed to result from the partial contact of the rubbing interface by GnP. Therefore, GnP can reduce friction and wear above 600 °C. The lubrication effect of GnP is believed to be closely related to its coverage on the sliding interface. The Raman mapping is mainly used to identify the coverage of GnP on the worn surface. As D, G, and 2D are the main identificial peaks of GnP, they were measured in this work. The D peak is related to the disordered structure of GnP, G is the characteristic peak of graphitic material, and D also reflects the sp^2 carbon material.

The Raman mapping of D ($1,350 \text{ cm}^{-1}$), G ($1,580 \text{ cm}^{-1}$), and 2D ($2,700 \text{ cm}^{-1}$) (red represents the highest intensity and blue represents the lowest intensity) in Figs. 5(a₂), 5(b₂), 6(a₂), 6(b₂), 11(a₂), 11(b₂), and 11(c₂) present the coverage state of GnP on the worn surface. Figures 5(a₁)–5(a₃) show the results at 600 °C. The strong G peak ($1,577 \text{ cm}^{-1}$) at red (A1) and green (A2) regions indicate that the GnP remains the layered structure, with a ratio of the intensities of D and G peaks (I_D/I_G) of 0.35 and 0.87 at A1 and A2 in Fig. 5, respectively. The G and 2D peaks, reflecting the graphite sp^2 can still be observed at A3, indicating that the GnP is almost totally covered on the wear track for the test at 600 °C. For the wear track at 700 °C (Figs. 5(b₁)–5(b₃)), the intensity of the G and 2D peaks becomes weaker, the I_D/I_G are 1.05, 5.5, and 9.9 at B1, B2, and B3, respectively, which suggests an increased defects of the GnP on the worn surface. The existence of G and 2D peaks indicates that the worn surface is still mostly covered by GnP, which explains the smooth COF curve and a reduced COF shown in Figs. 2(a) and 2(b).

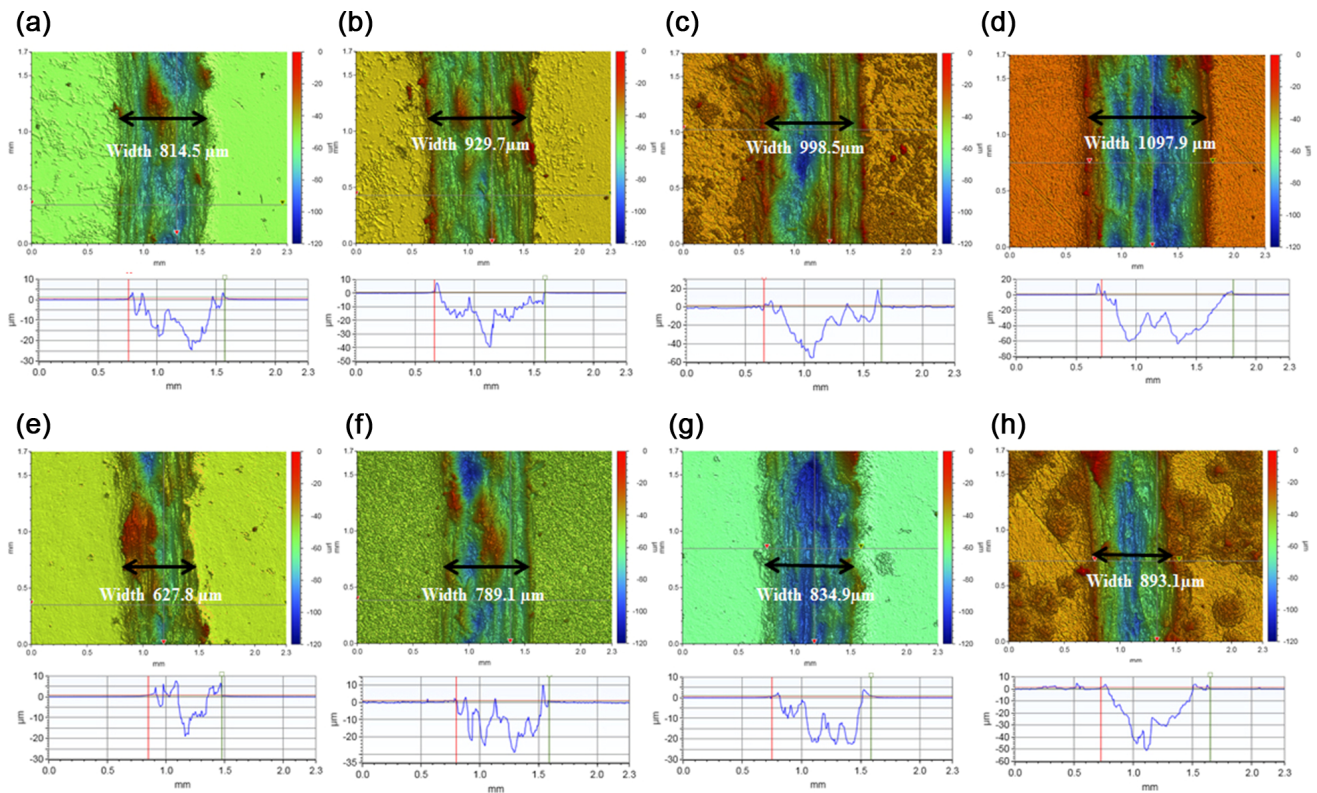


Fig. 4 3D morphologies and cross-sectional profile of the disc after tests at different conditions: un lubricated at (a) 600 °C, (b) 700 °C, (c) 800 °C, and (d) 900 °C; graphene lubricated at (e) 600 °C, (f) 700 °C, (g) 800 °C, and (h) 900 °C.

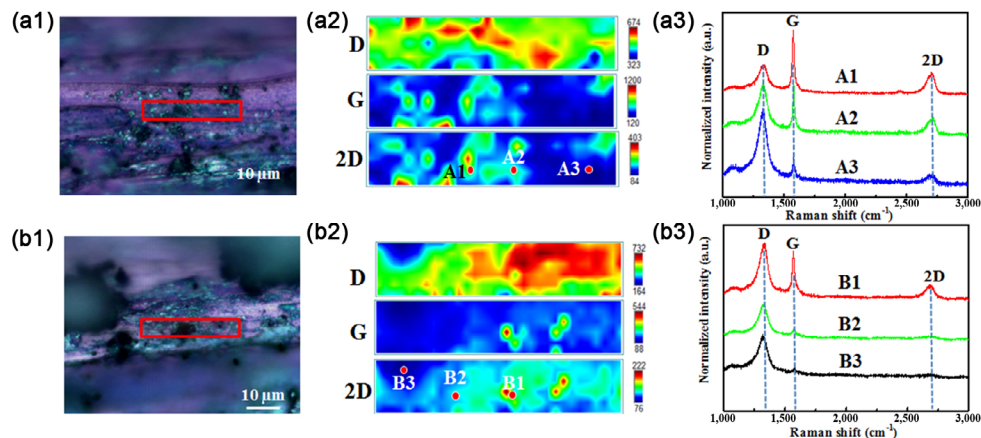


Fig. 5 Optical image and Raman mappings of the D, G, and 2D peaks, as well as the representative Raman spectrums of the worn surface of the disc after tests at (a₁–a₃) 600 °C and (b₁–b₃) 700 °C.

When it comes to 800 °C, the only limited red region (C1) shows the existence of a weak G and 2D peaks of GnP (Fig. 6(a₃)), and the I_D/I_G is 11, indicating that the limited GnP contains a large number of defects. Moreover, the regions C2 and C3 showing negligible G and 2D peaks suggest that little GnP was left on the worn surface. High temperature atmosphere can lead to the consumption of GnP due to oxidative

erosion of the graphene surface through gaseous CO and CO₂ [28]. It is reported that O₂ nucleates etch pits occur at temperatures above 875 °C for triple or thicker-layer graphene [29]. This oxidation occurs not only in the defect regions with lower activation barriers, but also on the pristine basal plane. The defects will significantly increase the oxidation reactivity at the rubbing interface. The high temperature, pressure,

and shear will produce some structural deformation, like some ripples and local bonding distortions, thus the oxidation etching will occur more easily. Therefore, at 800 °C, friction reduction can last for 70 s, some of the GnP was transformed into gaseous CO and CO₂, and released into the atmosphere [30]. The disappearance of GnP will lead to the direct contact of the rubbing interface, so the COF curve approaches the unlubricated sliding test results. At 900 °C, the Raman spectra (Fig. 6(b₃)) with negligible G and 2D peaks at all the regions of D1, D2, and D3 reveal that almost no residual GnP is present on the wear track surface. This stems from the heavy oxidation of graphene into gases after its exposure at 900 °C for a long period (10 min). The friction and wear results (Figs. 2(d) and 3) suggest that GnP is effective to provide lubrication for a short time (40 s at 900 °C), and the loss of lubrication results from the disappearance of GnP.

Due to oxidation of the GnP and its transformation into gas, GnP disappears after long exposure at high temperature, part of the GnP consumption could also result from the normal oxidation of graphene with oxygen group. Although graphene can be oxidized to some extent with oxygen functional groups in the edge and defect areas, it can still keep lubrication effects as graphene oxide are also promising lubricants [31, 32]. To prove this point, the commercial GnP was heat-treated at various temperatures (600, 700, 800, and 900 °C for 2 min), and then used as lubricant in friction tests at room temperature for 6 min. As shown in

Fig. 7, the COF fluctuates between 0.5 and 0.8 for unlubricated test during the whole sliding period. In the running period, the COF initially decreases from 0.8 to the lowest point at around 0.45, then climbs up to 0.6 after 80 s sliding. After adding GnP (5 mg) on the wear track, the COF remains stable at around 0.09 during the whole test period. Compared with unlubricated sliding test, above 80% reduction of COF was achieved when GnP was added, and the wear rate of the disc reduces more than 76%. The 2D cross-sectional profile of the wear scar of the discs in Fig. 8(d) is in agreement with the wear rate results, with a shallower wear scar for the GnP added condition compared with the unlubricated test. This reduction of friction and wear can be found for all GnP added conditions. As can be seen in Fig. 8, the width of the wear track on the disc for unlubricated test is around 591.2 μm, much larger than that of the GnP added condition, which is only around 380 μm. The diameters of the ball wear scar for GnP lubricated condition are from 312.16 to 352.9 μm, much smaller than that of the unlubricated test result (552.5 μm). The difference in the size of the wear scar for the plate and the ball results from the difference of the Hertz contact pressure, the ball suffers higher pressure and stays in contact all the time, while the plate is in contact periodically [20]. The above results suggest that heat-treated GnP still has a comparable lubrication effect even though high temperature is supposed to produce some oxidation of graphene with oxygen and supposedly affect the lubricating properties of GnP. This can be

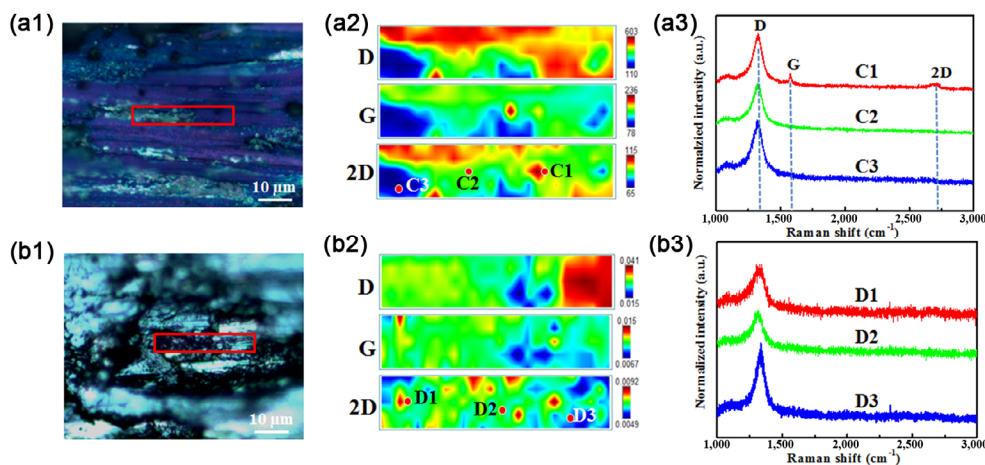


Fig. 6 Optical images and Raman mappings of the D, G, and 2D peaks, as well as the representative Raman spectra of the worn surface of the disc after tests at (a₁–a₃) 800 °C and (b₁–b₃) 900 °C.

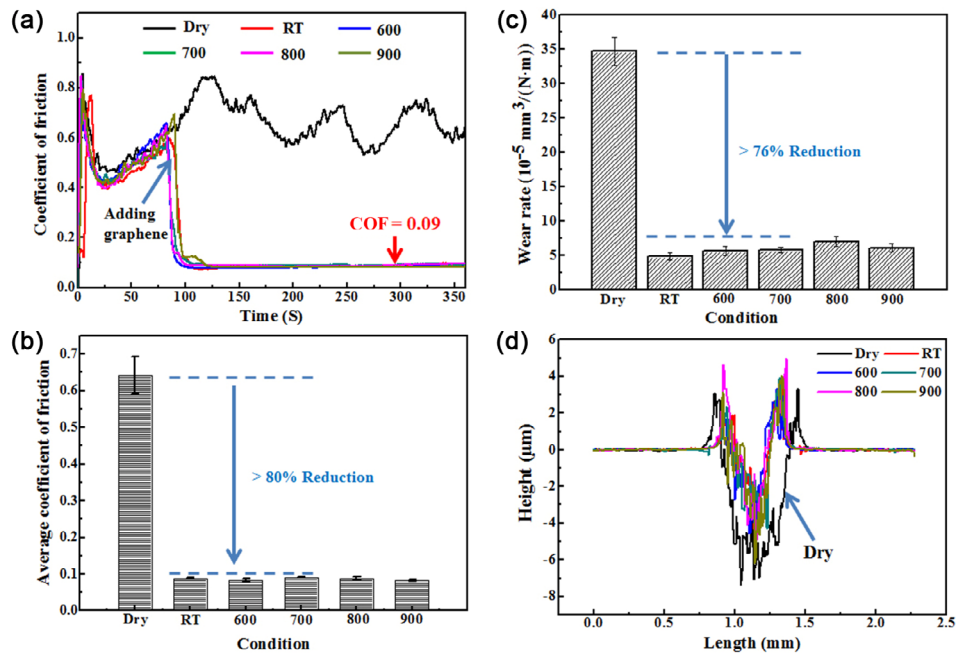


Fig. 7 Tribological results tested at room temperature. (a) COF as a function of time with the heat-treated GnP added after 85 s of unlubricated sliding, entire unlubricated sliding test was also given as a comparison; (b) average COF for the steady period (after 100 s). (c) Wear rate and (d) 2D profile of the wear track of the discs at different temperature.

explained by the fact that although high temperature exposure of graphene will lead to an increase of defect, it still remains a layered structure to separate the direct contact of the rubbing interface, thus reduces friction and wear.

To better demonstrate the effect of GnP as lubricant for hot rolling, results with GnP as lubricant assessed using the hot rolling mill were also shown in Fig. 9. Lubrication effects of lubricant for hot rolling process are correlated with rolling force, the better is the lubrication (lower friction), the lower is the rolling force. Figure 9 shows the rolling force and the average surface roughness of the strip surface after the rolling experiments with water and GnP lubrication conditions at different temperatures (the samples are heat-treated at 950, 1,050, and 1,150 °C for 25 min). It is clear that the rolling force is lower for the GnP lubricated condition compared with that of water lubricated tests. The average rolling force for water lubricated is 242.5, 214.5, and 170.8 kN for the steel samples heat-treated at 950, 1,050, and 1,150 °C, respectively. GnP contributes to about 11%, 7.4%, and 6.9% reduction in rolling force for tests at these three temperatures, respectively, with the rolling force reduced to 215.7, 198.7, and 158.9 kN, respectively. As shown in Fig. 9(b),

the average roughness of the rolled samples after GnP lubrication is slightly lower compared to the pure water lubricated condition. These results suggest that GnP can provide lubrication for the hot rolling process at 950 °C, which is in agreement with the above laboratory ball-on-disc results.

Figure 10 shows 3D morphologies and 2D profile of the rolled sample surface under water and GnP lubrication conditions. Some defects can be found on the rolled surface under water lubricated condition, such as cracks and scratches on the rolled surface shown in Figs. 10(a) and 10(b), and the corresponding roughness curves show large fluctuation. These defects and rough surface indicate the poor lubrication of water. Under the GnP lubricated condition, the rolled surface becomes smoother without apparent cracks, and the fluctuation of the corresponding roughness was not as significant as that of the water lubricated surface.

Raman mapping and spectra of the rolled sample surface lubricated by GnP are shown in Fig. 11. The typical D, G, and 2D peaks at around 1,350, 1,580, and 2,700 cm⁻¹ respectively are correlated to the carbon, which indicates that GnP stays on the rolled sample surface. For the results at 950 °C (Fig. 11(a₃)), besides

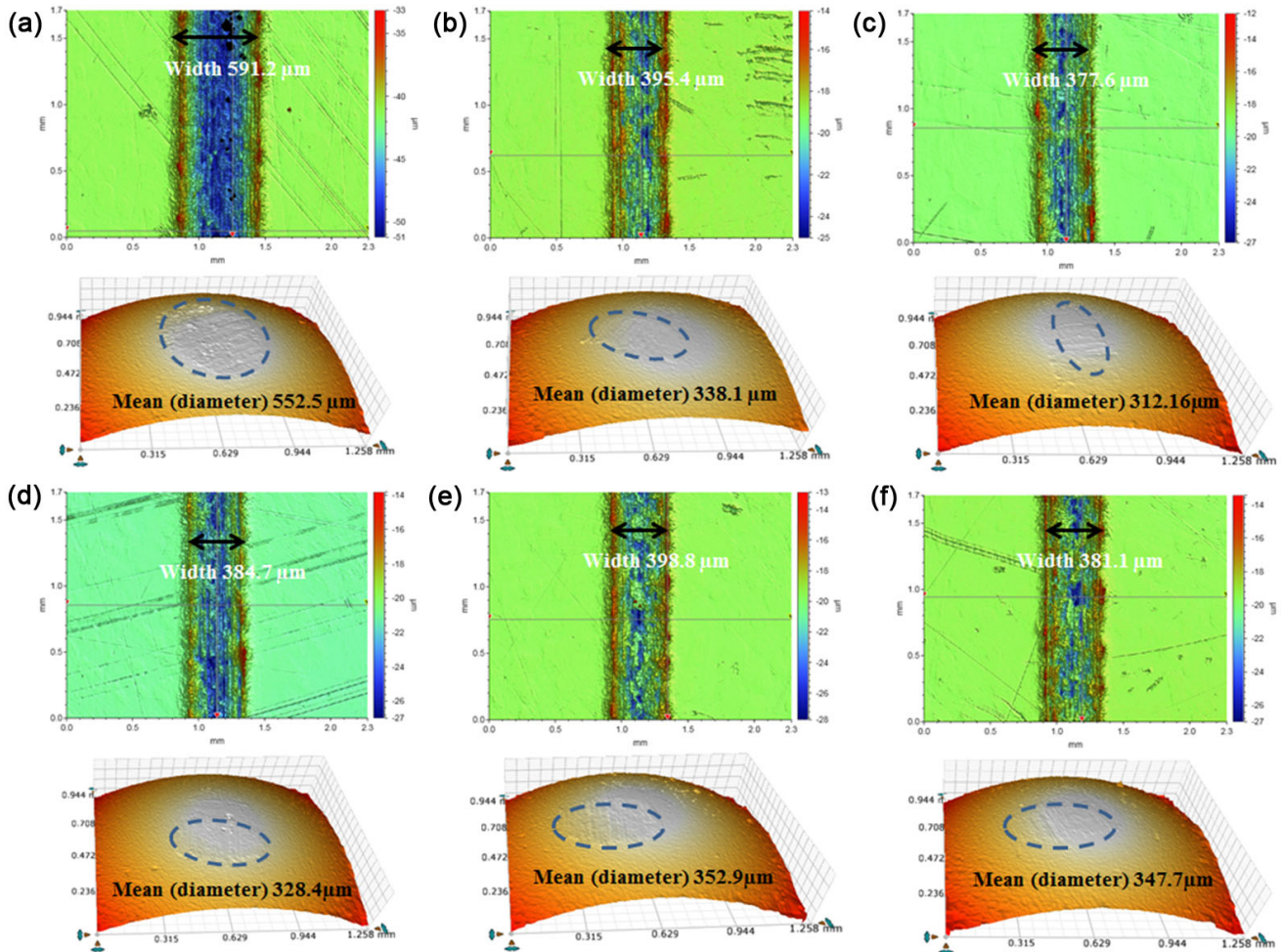


Fig. 8 3D morphologies of the wear track of the disc and ball after tested at different conditions: (a) unlubricated test; (b) commercial GnP non heat-treated; (c) GnP heat-treated at 600 °C; (d) GnP heat-treated at 700 °C; (e) GnP heat-treated at 800 °C; and (f) GnP heat-treated at 900 °C.

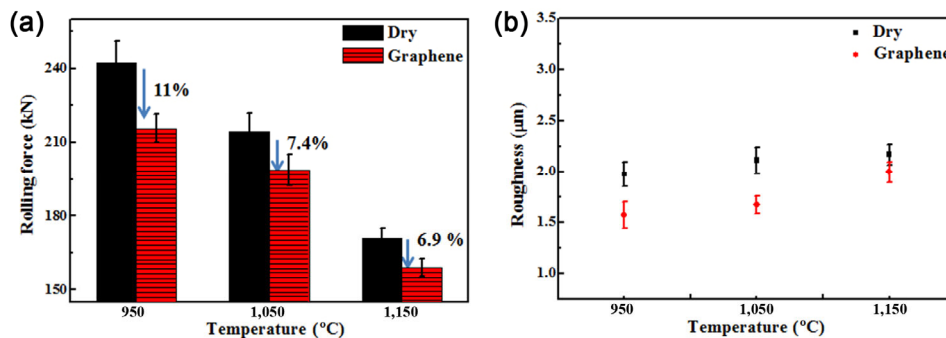


Fig. 9 (a) Rolling force as a function of temperature for GnP lubricated result and water lubricated tests. (b) Average roughness of the rolled sample surface.

the strong G and 2D peaks at A1, weaker D and G peaks can also be identified at region A2 and A3, and the I_D/I_G at the regions of A1, A2, and A3 are 0.24, 1.2, and 4.1, respectively. At 1,050 °C (Fig. 11(b₃)), weak G peaks can also be observed at the regions of B1, B2,

and B3, and the corresponding I_D/I_G are 1.1, 2.9, and 5.3, respectively. At 1,150 °C, results from Fig. 11(c₃) indicate there also exist weak G peaks in regions C1 and C2, with the I_D/I_G ratio of 4.9 and 3.1 respectively. Negligible G and 2D peaks at C3

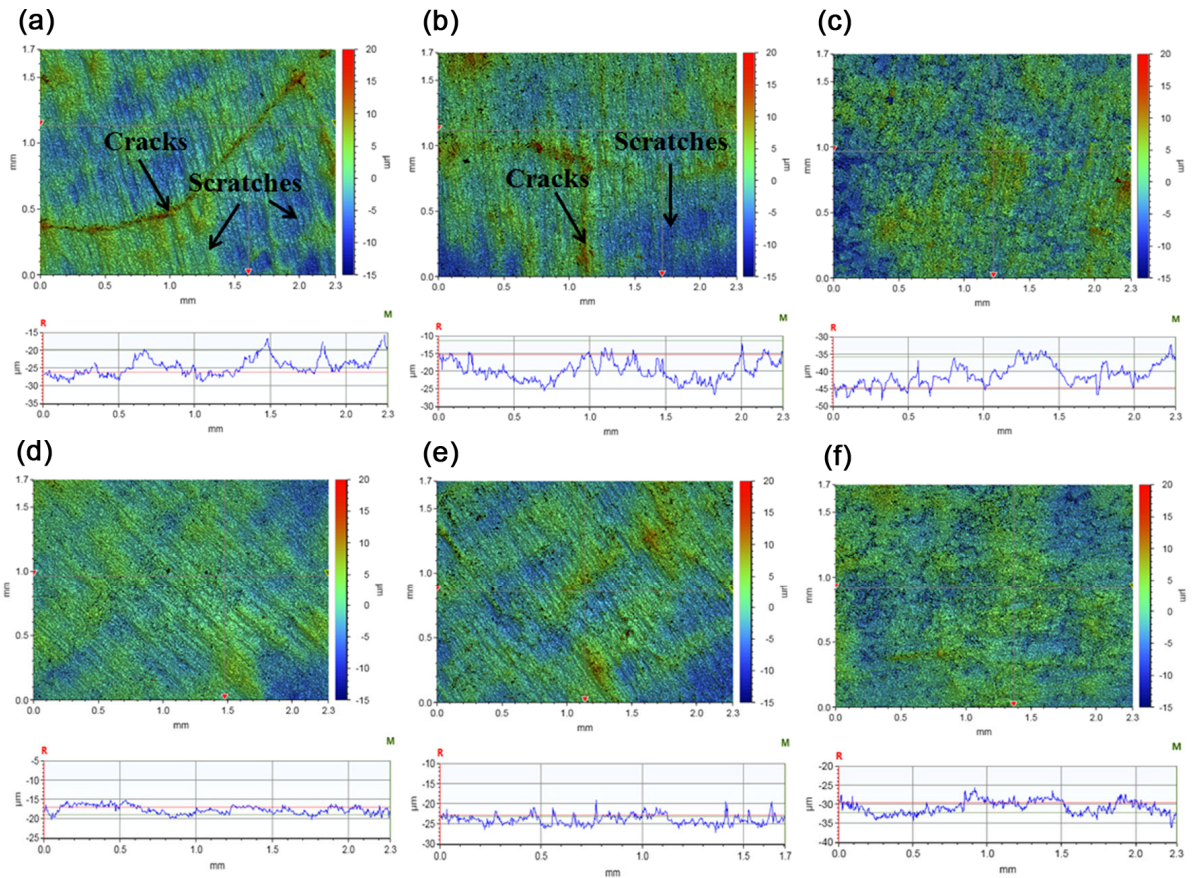


Fig. 10 3D morphologies and 2D profile of the rolled samples: water lubricated at (a) 950 °C, (b) 1,050 °C, and (c) 1,150 °C; GnP lubricated at (d) 950 °C, (e) 1,050 °C, and (f) 1,150 °C.

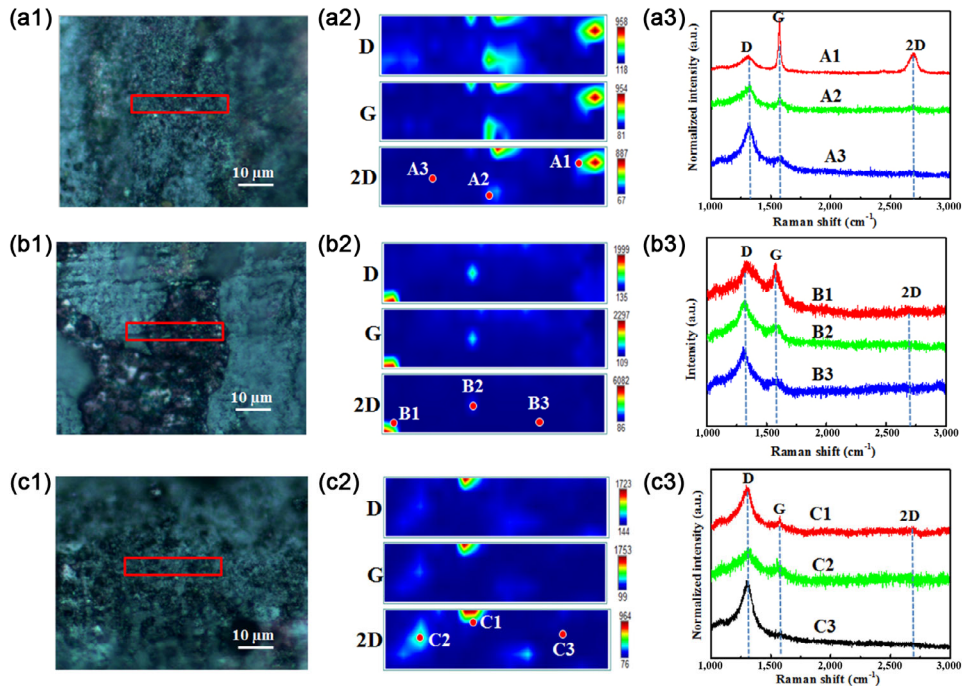


Fig. 11 Optical image, Raman mapping of D, G, and 2D of the corresponding marked red box region and the representative Raman spectrums for the rolled samples surface with GnP as lubricant at different temperatures: (a₁–a₃) 950 °C; (b₁–b₃) 1,050 °C; and (c₁–c₃) 1,150 °C.

(large blue region) suggest that reduced GnP can be found on the rolled sample surface. Generally, the I_D/I_G increases with temperature (taking A1 at 950 °C, B1 at 1,050 °C, and C1 at 1,150 °C for examples), which indicates an increased defects of the GnP with higher temperatures. The protective GnP prevents the direct contact between the hot strip and roller, thus reduces the friction and rolling force. At the rolling interface, the temperatures are around 795, 890, and 960 °C for the samples heat-treated at 950, 1,050, and 1,150 °C, respectively (measured by Micro IR-1200 non-contact infrared thermometer).

The TGA results of GnP shown in Fig. 12 suggest that GnP loses weight sharply at the temperature of 650 °C. Considering the short contact period (10^{-3} – 10^{-2} s) for the hot rolling process, the GnP still maintains a layered structure and provides lubrication, and the increase of temperature will increase the O_2 nucleation etch pits area. More defects are also more likely to be introduced into the graphene sheets after experiencing the high loading and shearing of the hot rolling process. It is reported that continuous O_2 nucleation etch pit occurs at 875 °C and above for the graphene with the layers above three [29]. The lower contact temperature (around 795 °C) for the samples heat-treated at 950 °C (much lower than the continuous O_2 nucleation temperature) is not high enough to oxidize the graphene significantly, so the GnP with lower oxidation defects retains the graphitic (layered) structure after cooling down. This layered structure is attributed to the reduction of rolling force to around 11%, as can be seen in Fig. 9(a). For the higher contact temperatures around 890 and 960 °C, more O_2 oxidation nucleation pits occur, however, the short contacting time is not long enough to oxidize the graphene totally. The GnP can still maintain the layered structure with some internal defects, thus contributes to the rolling force reduction. It is reported that it is difficult for the graphite to be ignited even with a naked flame at 1,000 °C, due to its promising high thermal conductivity [4, 33]. GnP is also likely to transfer the heat from the strip to the roller (It should be noted that the strip is heated to an elevated temperature whereas the roll surface temperature is at room temperature at the start of the rolling test), and keep itself layered structure at high temperature for a short period. Compared with the rolling force

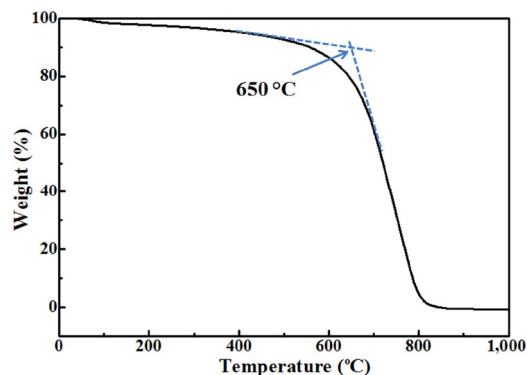


Fig. 12 TGA results of GnP conducted in air with a heating rate of 20 °C/min.

reduction of 11% at 795 °C, those at 890 and 960 °C are slightly lower, around 7.4% and 6.9%, respectively, due to the partially deterioration of the graphene layer. Because it still needs around 1–2 min for the rolled sample to cool down below 700 °C, the residual GnP on the rolled sample surface will be continuously oxidated and gasified into CO_2 [30], leading to a weak G peak, as shown in Fig. 11. The further oxidation, especially the gasification of GnP is supposed to produce the black contamination of traditional black lubricant. The results of laboratory ball-on-disc and hot rolling apparatus show some disparity, where the friction reduction seems negligible at the 900 °C for ball-on-disc test, however, the achieved reduction of rolling force can still reach 6.7% at 960 °C for the hot rolling tests. Although some residual GnP was identified on the hot rolled strips, it is negligible on the counterparts for ball-on-disc samples. The difference results from two aspects, contact time difference and temperature difference. The introduced GnP for ball-on-disc was heated at the sliding interface for hundreds of seconds under relatively low sliding speed (0.01 m/s); during hot rolling, it was only 10^{-3} – 10^{-2} s, and this short time was insufficient to oxidize the GnP totally, thus GnP still kept the layered structure and functions effectively even at the temperature of 960 °C. For ball-on-disc test, to exclude the effect of water under high temperature, the GnP was directly introduced into the wear track without any water, thus the GnP was heated immediately. However, for the hot rolling tests, the GnP was introduced with water, and the cold roll was heated, the heat in the hot strip was partly transferred by the water and delayed the oxidation of GnP. In practice,

however, the temperature of the hot strip is high (950 °C), the maximum temperature of the roller is only 650 °C, so the average temperature of the GnP of 800 °C between the above two temperatures is still within the effective lubrication range of MLG. So, it is considered that GnP can be used as hot metal forming lubricant, the oxidation and gasification after its lubrication at high temperature is likely to ease the environmental black contamination from the traditional graphite based lubricant.

The 2D planar structure with weak van der Waals forces between the layers of GnP results in a lower frictional resistance compared with the unlubricated condition. The coverage of GnP is vital for the lubrication effect. At 600 °C, the worn surface is still covered by layered GnP, whereas a reduced coverage of the GnP at higher temperatures is responsible for the failure of lubrication. A higher temperature will lead to increased oxidative erosion and defects of the GnP, and even make it decompose at 900 °C.

In this study, it is found that the lubrication effect of GnP is closely related to temperatures and working conditions. Below 600 °C, GnP can provide stable lubrication. Above 600 °C, GnP can still be used as lubricant for some hot working conditions, where the rubbing counterpart is in contact for a short duration, such as sheet metal forming, the contact time of which is only 10^{-3} – 10^{-2} s. As the lubrication mechanism is the easily sheared GnP, lubrication effect can be obtained if the GnP is located in the rubbing interface without destruction. So, it is believed that it is also possible for GnP to provide lubrication for bulk forming, such as hot forging and hot extraction, where the contact time is short. And the pressure (a few GPa) is unlikely to destroy the layered structure of GnP. The tests in this study are conducted at 0.1 m/s and 0.8 GPa. Under the higher speed forming and pressure conditions, it is believed that GnP can also function well. But, whether there exist thresholds of pressure and speed for promising lubrication of GnP needs be explored in the future. As the extreme pressure exceeds the strength of GnP, the GnP can be possibly destroyed and lose the lubrication, and the extreme high speed with thermal effect can cause the local oxidation of GnP, which is also supposed to influence the lubrication of GnP.

4 Conclusions

This work studies the potential of graphene used as lubricant at high temperatures above 600 °C using both ball-on-disc tribo-meter and hot rolling mill, although graphene is supposed to lose its lubrication effectiveness above 600 °C. The ball-on-disc results suggest that below 700 °C, the added GnP can provide lubrication more than 3 min. At the higher temperatures above 800 °C, GnP is still effective in lubrication for 40 s. The loss of lubrication for long durations of tests results from the gasification of GnP, due to the oxidation at the pressure and shear induced defects areas at high temperatures. Several minutes of lubrication of GnP above 800 °C is still effective for some working conditions, like hot rolling. Although the working temperature is high (around 950 °C), the short rolling contact time 10^{-3} – 10^{-2} s is not long enough for the gasification of GnP. The hot rolling results confirm the effectiveness of graphene as lubricant at the temperature from 795 to 960 °C, the rolling force reduction can reach 11% at 795 °C, about 7.4% and 6.9% at 890 and 960 °C, respectively. Therefore, it can be concluded that for a short contact time, GnP still maintains its layered structure and can provide an effective lubrication regime, even up to 960 °C. The oxidation and gasification after its lubrication at high temperatures are likely to ease the environmental contamination from the traditional graphite based lubricant. This character makes graphene a potential high temperature lubricant for the hot metal forming process.

Acknowledgements

This work was supported by the Australian Research Council Discovery Project (No. DP190103455) and the Linkage Project (No. LP160101871). The authors thankfully acknowledge the assistance of Mr. Maosheng Chai at Tsinghua University to conduct the Raman mapping analysis.

Open Access This article is licensed under a Creative Commons Attribution 4.0 International License, which permits use, sharing, adaptation, distribution and reproduction in any medium or format, as long as

you give appropriate credit to the original author(s) and the source, provide a link to the Creative Commons licence, and indicate if changes were made.

The images or other third party material in this article are included in the article's Creative Commons licence, unless indicated otherwise in a credit line to the material. If material is not included in the article's Creative Commons licence and your intended use is not permitted by statutory regulation or exceeds the permitted use, you will need to obtain permission directly from the copyright holder.

To view a copy of this licence, visit <http://creativecommons.org/licenses/by/4.0/>.

References

- [1] Novoselov K S, Geim A K, Morozov S V, Jiang D, Zhang Y, Dubonos S V, Grigorieva I V, Firsov A A. Electric field effect in atomically thin carbon films. *Science* **306**(5696): 666–669 (2004)
- [2] Lee C, Wei X, Kysar J W, Hone J. Measurement of the elastic properties and intrinsic strength of monolayer graphene. *Science* **321**(5887): 385–388 (2008)
- [3] Zhang Y, Tan Y W, Stormer H L, Kim P. Experimental observation of the quantum Hall effect and Berry's phase in graphene. *Nature* **438**(7065): 201–204 (2005)
- [4] Balandin A A, Ghosh S, Bao W, Calizo I, Teweldebrhan D, Miao F, Lau C N. Superior thermal conductivity of single-layer graphene. *Nano Lett* **8**(3): 902–907 (2008)
- [5] Wang X, Zhi L, Müllen K. Transparent, conductive graphene electrodes for dye-sensitized solar cells. *Nano Lett* **8**(1): 323–327 (2008)
- [6] Wang S, Zhang Y, Abidi N, Cabrales L. Wettability and surface free energy of graphene films. *Langmuir* **25**(18): 11078–11081 (2009)
- [7] Kim K S, Lee H J, Lee C, Lee S K, Jang H, Ahn J H, Kim J H, Lee H J. Chemical vapor deposition-grown graphene: The thinnest solid lubricant. *ACS Nano* **5**(6): 5107–5114 (2011)
- [8] Berman D, Erdemir A, Sumant A V. Graphene: A new emerging lubricant. *Mater Today* **17**(1): 31–42 (2014)
- [9] Holmberg K, Andersson P, Erdemir A. Global energy consumption due to friction in passenger cars. *Tribol Int* **47**: 221–234 (2012)
- [10] Alberts M, Kalaitzidou K, Melkote S. An investigation of graphite nanoplatelets as lubricant in grinding. *Int J Mach Tools Manuf* **49**(12–13): 966–970 (2009)
- [11] Marchetto D, Restuccia P, Ballestrazzi A, Righi M C, Rota A, Valeri S. Surface passivation by graphene in the lubrication of iron: A comparison with bronze. *Carbon* **116**: 375–380 (2017)
- [12] Liang S, Shen Z, Yi M, Liu L, Zhang X, Ma S. *In-situ* exfoliated graphene for high-performance water-based lubricants. *Carbon* **96**: 1181–1190 (2016)
- [13] Hu Y, Wang Y, Zeng Z, Zhao H, Ge X, Wang K, Wang L, Xue Q. PEGlated graphene as nanoadditive for enhancing the tribological properties of water-based lubricants. *Carbon* **137**: 41–48 (2018)
- [14] Du S, Sun J, Wu P. Preparation, characterization and lubrication performances of graphene oxide–TiO₂ nanofluid in rolling strips. *Carbon* **140**: 338–351 (2018)
- [15] Puértolas J A, Castro M, Morris J A, Ríos R, Ansón-Casaos A. Tribological and mechanical properties of graphene nanoplatelet/PEEK composites. *Carbon* **141**: 107–122 (2019)
- [16] Zhou H, Wang H, Du X, Zhang Y, Zhou H, Yuan H, Liu H Y, Mai Y W. Facile fabrication of large 3D graphene filler modified epoxy composites with improved thermal conduction and tribological performance. *Carbon* **139**: 1168–1177 (2018)
- [17] Han H, Meng F, Yang C. Investigating tribological performances for GNPs/MoS₂ coating at variable temperatures. *Tribol Lett* **66**(3): 1–13 (2018)
- [18] Song H, Ji L, Li H, Wang J, Liu X, Zhou H, Chen J. Self-forming oriented layer slip and macroscale super-low friction of graphene. *Appl Phys Lett* **110**(7): 073101 (2017)
- [19] Shen B, Hong H, Chen S, Chen X, Zhang Z. Cathodic electrophoretic deposition of magnesium nitrate modified graphene coating as a macro-scale solid lubricant. *Carbon* **145**: 297–310 (2019)
- [20] Berman D, Erdemir A, Sumant A V. Reduced wear and friction enabled by graphene layers on sliding steel surfaces in dry nitrogen. *Carbon* **59**: 167–175 (2013)
- [21] Berman D, Erdemir A, Sumant A V. Few layer graphene to reduce wear and friction on sliding steel surfaces. *Carbon* **54**: 454–459 (2013)
- [22] Savvatimskiy A I. Measurements of the melting point of graphite and the properties of liquid carbon (a review for 1963–2003). *Carbon* **43**(6): 1115–1142 (2005)
- [23] Xu Z, Zhang Q, Jing P, Zhai W. High-temperature tribological performance of TiAl matrix composites reinforced by multilayer graphene. *Tribol Lett* **58**(1): 3 (2015)
- [24] Xiao Y, Shi X, Zhai W, Yang K, Yao J. Effect of temperature on tribological properties and wear mechanisms of NiAl matrix self-lubricating composites containing graphene nanoplatelets. *Tribol Trans* **58**(4): 729–735 (2015)
- [25] Zhu Q, Zhu H T, Tieu A K, Reid M, Zhang L C. *In-situ* investigation of oxidation behaviour in high-speed steel roll material under dry and humid atmospheres. *Corros Sci* **52**(8): 2707–2715 (2010)



- [26] Kato O, Yamamoto H, Ataka M, Nakajima K. Mechanisms of surface deterioration of roll for hot strip rolling. *ISIJ Int* **32**(11): 1216–1220 (1992)
- [27] Jourani A, Bouvier S. Friction and wear mechanisms of 316L stainless steel in dry sliding contact: Effect of abrasive particle size. *Tribol Trans* **58**(1): 131–139 (2015)
- [28] Xu S C, Irle S, Musaev D G, Lin M C. Quantum chemical study of the dissociative adsorption of OH and H₂O on pristine and defective graphite (0001) surfaces: Reaction mechanisms and kinetics. *J Phys Chem C* **111**(3): 1355–1365 (2007)
- [29] Liu L, Ryu S, Tomasik M R, Stolyarova E, Jung N, Hybertsen M S, Steigerwald M L, Brus L E, Flynn G W. Graphene oxidation: Thickness-dependent etching and strong chemical doping. *Nano Lett* **8**(7): 1965–1970 (2008)
- [30] Jia Y, Wan H, Chen L, Zhou H, Chen J. Effects of phosphate binder on the lubricity and wear resistance of graphite coating at elevated temperatures. *Surf Coat Technol* **315**: 490–497 (2017)
- [31] Kinoshita H, Nishina Y, Alias A A, Fujii M. Tribological properties of monolayer graphene oxide sheets as water-based lubricant additives. *Carbon* **66**: 720–723 (2014)
- [32] Gupta B, Kumar N, Panda K, Kanan V, Joshi S, Visoly-Fisher I. Role of oxygen functional groups in reduced graphene oxide for lubrication. *Sci Rep* **7**(1): 45030 (2017)
- [33] He Y, Zhang N, Wu F, Xu F, Liu Y, Gao J. Graphene oxide foams and their excellent adsorption ability for acetone gas. *Mater Res Bull* **48**(9): 3553–3558 (2013)



Long WANG. He received his M.S. degree in 2017 from Lanzhou Institute of Chemical Physics, Chinese Academy of Sciences. In 2021, he obtained his Ph.D. degree

in University of Wollongong, Australia. His research interest is high-temperature tribology and lubrication, self-lubricating materials, and tribology under extreme conditions.



Anh Kiet TIEU. He is a senior professor at University of Wollongong. In 2007, He was to be an academician of Australian Academy of Technological Sciences and Engineering.

He was awarded the William Johnson International Gold Medal in 2012 for lifetime achievements in materials processing research and teaching. His research areas cover tribology, lubrication, rolling technology, and computational mechanics.



Hongtao ZHU. He is an associate professor at University of Wollongong, Australia. He received his Ph.D. degree from Northeastern University, China, in 2000. He was a postdoc with Shanghai Jiao Tong University, China for two years, and

joined the University of Wollongong in 2002. His research interests include tribology, contact mechanics, oxidation, quantum, and molecular dynamic simulation. He leads research themes on “Contact mechanics and damage of wheel and rail system” and “Computational modelling in tribology” at University of Wollongong.